Talanta 100 (2012) 27–31

Contents lists available at SciVerse ScienceDirect

Talanta

journal homepage: www.elsevier.com/locate/talanta

Signal-to-noise ratio enhancement of the compact light-emitting diode-induced fluorescence detector

Xuhui Geng [a,b], Dapeng Wu [a], Qian Wu [a,b], Yafeng Guan [a,*]

[a] Department of Instrumentation and Analytical Chemistry, Key Lab of Separation Science for Analytical Chemistry of CAS, Dalian Institute of Chemical Physics, Chinese Academy of Sciences, 457 Zhongshan Road, Dalian 116023, China
[b] Graduate School of the Chinese Academy of Sciences, Beijing 100039, China

ARTICLE INFO

Article history:
Received 30 May 2012
Received in revised form
14 August 2012
Accepted 27 August 2012
Available online 2 September 2012

Keywords:
Light-emitting diode
Fluorescence detector
SNR enhancement
Compact

ABSTRACT

To enhance the SNR (signal-to-noise ratio) of the compact light-emitting diode-induced fluorescence detector (LED-FD) ([14]), key parameters including LED and its coupling style, pinhole diameter, calibration, and refractive index matching fluid (RIMF) were optimized. A 20 mA LED with light intensity of 8400 mcd was used as new light source. To optimize pinhole diameter, a theoretical analysis based on a three-dimensional (3D) view of the detection area was proposed and validated experimentally. A calibration principle from the 3D perspective was proposed. The detection flow cell and the collection fiber were adjusted to be coplanar. RIMF (glycerol) was applied to enhance SNR. The performance of the improved LED-FD was evaluated by flow injection analysis (FIA). The limit of detection (LOD) was determined as 0.15 nM sodium fluorescein (SNR=3). Compared with our previous work, a five-fold enhancement on the SNR was obtained. The LOD was about five times higher than that of commercial Agilent G1321A FLD which employed a xenon pulse lamp.

1. Introduction

Fluorescence detection has been one of the most sensitive and selective detection schemes available for fluid flow systems, such as flow injection analysis (FIA), capillary electrophoresis (CE), and liquid chromatography (LC) [1–3]. The light-emitting diode (LED) has many prominent advantages, including low energy consumption, long lifetime, high stability, small size, and low cost. It is commercially available at wavelengths ranging from UV to near-IR regions [4], and its radiant power per square millimeter of the chip now can reach hundreds of milliwatts, which is high enough to induce fluorescence efficiently [5]. LEDs have been used as alternative light sources in fluorescence detection [6–8]. However, because of its area source and incoherent characteristic nature, it is difficult to focus an LED light beam to a spot in the range of hundreds of micrometers to match the size of a capillary inner diameter (i.d.). The light-emitting diode-induced fluorescence detectors (LED-FDs), therefore, exhibit a much higher limit of detection (LOD) than laser induced fluorescence detectors (LIFs).

Various methods were used to enhance the SNR (signal-to-noise ratio), including employment of HP (high power) LEDs, pulse driven LEDs, lenses and microscopes, objectives, etc. [9,10]. Among them, the lowest LOD was 3 pM which was obtained by de Jong and Lucy [9]. They used a 700 mW HP LED. The LED was first focused by an aspheric lens, and then by a 20× microscope objective. Fluorescence was also collected by a 20× microscope objective. The LOD was evaluated by continuous flow measurements with a 200 μm i.d. capillary. To our knowledge, except in this work, LODs of most LED-FDs reported so far were at the nano molar level [11–13]. The value next to the lowest was 0.29 nM which was reported by Dan Xiao's group [10]. In their work, the rate currents of 20 mA of two LEDs were pulsed to 200 mA. The LEDs were focused by lenses on a GRIN lens which was coupled to a fiber inserted into the capillary detection cell (end part of a CE column). Fluorescence was collected by a 60× microscope objective. The LOD was evaluated by a CE system with a 75 μm i.d. capillary. These setups increased the size and complexity of the detector.

The aim of our study was to develop a compact, robust, and sensitive LED-FD detector which could be easily fabricated, replicated, and steadily applied to fluorescence detection of micro flow systems. No sophisticated or bulk optical devices were employed. Along this route, our group recently developed a compact LED-FD with an LOD of 0.75 nM [14]. An ordinary LED, an excitation filter and a pinhole were integrated in a canister in direct contact with each other, without any lens or fiber coupling.

Abbreviations: GRIN, Gradient index; FITC, Fluorescein isothiocyanate; PMT, Photomultiplier tube; FWHM, Full wave at half maximum; RIMF, Refractive index matching fluid.

* Corresponding author. Tel.: +86 411 84379570; fax: +86 411 84379590.
E-mail addresses: guan_yafeng@yahoo.com.cn, kfguan@mail.dlptt.ln.cn (Y. Guan).

0039-9140/$ - see front matter © 2012 Elsevier B.V. All rights reserved.
http://dx.doi.org/10.1016/j.talanta.2012.08.043

A screw back was used for impacting. The LOD was evaluated by FIA with a capillary flow cell of 250 μm i.d. The LOD value of 0.75 nM was already among the lowest in literature [11–13].

In order to further enhance the SNR, the four parameters, i.e., LED and its coupling style, the pinhole diameter, calibration, and refractive index matching fluid (RIMF), were further investigated and improved. For each parameter, detailed theoretical analysis and experimental result were given and matched well. An LOD of 0.15 nM (SNR=3) was achieved finally. Compared with our previous LED-FD [14], a five-fold enhancement on the SNR was obtained. The new detector was combined with an Agilent 1200 Series HPLC system to separate and detect four kinds of amino acids to demonstrate its applicability.

2. Experimental

2.1. Chemicals and reagents

Sodium fluorescein, arginine (Arg), valine (Val), leucine (Leu), phenylalanine (Phe) and FITC were purchased from Sigma, USA. The standard sample was dissolved and diluted with deionized (DI) water to required concentrations. Brown bottle containers were used to prevent sodium fluorescein from photodegrading. Deionized water was used throughout the experiments.

2.2. Apparatus and equipments

A FIA system was constructed to evaluate the performance of the LED-FD. A fused-silica capillary of 250 μm i.d., 365 μm o.d., with a 20 μm-polyimide coating (Xinnuo Optical Fiber Inc., Handan, China) was used, on which a 3 mm detection window was carefully burned and cleaned. A P230 HPLC pump (Elite Co. Ltd., Dalian, China) was used to pump the mobile phase. The mobile phase (deionized water) was degassed with ultrasound before use. Injection was performed using a six-port injection valve (Valco Instruments, Houston, TX, USA) with a 10 μL loop. Before the six-port injection valve, a commercial three-port manifold (SS316, 1/16 in, Dalian Elite Analytical Instruments Corp. Ltd., China) and a split were used to finely adjust the flow rate to 10 μL/min.

2.3. Optical systems

The optical arrangement of the LED-FD is shown in Fig. 1. A super blue LED (OSB56L3131A, OptoSupply Corp., Hong Kong, China) was used as excitation light source. Detailed parameters of the LED were: λ_{max} 470 nm, FWHM 25 nm, power dissipation 20 mA × 3.1 V, 50% power angle 30°, diameter 3 mm, and typical light intensity 8400 mcd. An interference filter (BP 470 nm, FWHM 20 nm; Huibo Optical Corp. Ltd., China) was used to eliminate the interference of long-wavelength light from the LED. A 350 μm-diameter pinhole was fabricated by punching on a 55 μm-thick black light tight adhesive tape (BTX-8923AD, Bitaixiang Electronic Corp. Ltd., China). The tape and flow cell were in physical contact. An optical fiber (quartz core diameter 300 μm, fluorine resin cladding 15 μm, length 45 mm, numerical aperture (NA) 0.37; Chunhui Inc., China) was used to collect fluorescence. The fluorescence passed through an interference filter (BP 530 nm, FWHM 30 nm; Huibo Optical Corp. Ltd., China), then was detected by a metal packaged mini PMT (H5784, Hamamatsu, Japan). The signal from the PMT was acquired by a chromatographic workstation N2000 (Zhejiang University, China). The system was based on orthogonal optical arrangement. The excitation path was perpendicular to the plane of flowcell and the fluorescence collection path. The angle between the flowcell and the collection fiber was 45°, which was demonstrated to be the optimum collection angle [15].

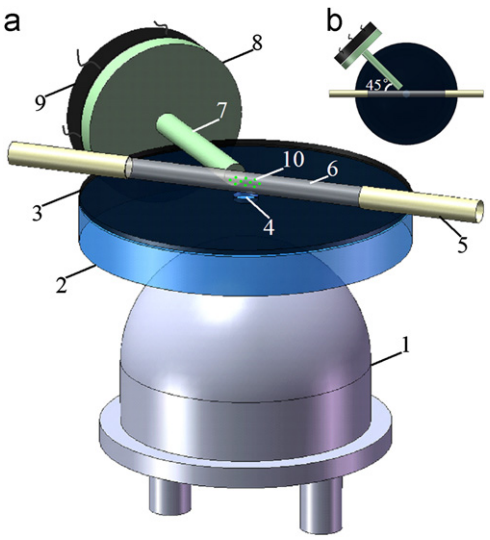

Fig. 1. Schematic diagram of the optical setup of the new LED-FD system. (a) 3D view and (b) top view. (1) LED; (2) excitation filter; (3) light tight adhesive tape; (4) pinhole; (5) fused-silica capillary; (6) detection window (flow cell); (7) collection fiber; (8) emission filter; (9) photomultiplier tube; and (10) excited fluorescence molecules.

2.4. Derivatization and separation of amino acids

The four amino acids were labeled and separated on the HPLC instrument. Each amino acid was prepared to a 4 mM stock solution by DI water. A FITC solution of 10 mM in acetone (containing 1% v/v pyridine) was used as the labeling reagent. $Na_2B_4O_7$ solution of 10 mM (pH 9.0) was used as buffer. Every 1.2 mM amino acid labeling solution was prepared by mixing 60 μL stock solution of each amino acid with 60 μL labeling reagent and 80 μL borate buffer, and the resultant mixture was left in the dark overnight at room temperature. Then the four 1.2 mM FITC-labeled amino acid stock solutions were diluted to 1.2×10^{-5} M with borate buffer, and mixed by equal volume. Working solutions were prepared by diluting the mixed stock with borate buffer. The separation was performed on a CenturySIL C18 300 A analytical column (150 mm × 4.6 mm × 5 μm, Johnsson Inc., Dalian, China) at room temperature. The mobile phases were: (A) 20 mM disodium (containing 5% v/v methanol, pH 8.84) and (B) methanol. The gradient elution program was: ~0–15 min, ~90% A–60% A. Other chromatographic conditions were: flow rate 0.75 mL min^{-1} and injection volume 20 μL.

3. Results and discussion

As an excitation light source, LED plays the most important role in an LED-FD. Its performance and coupling style contribute directly to the system SNR. The pinhole confined the passed area of the LED beam, and determined the amplitude of the induced fluorescence signal and scattered background noise [9]. The calibration of the pinhole, capillary flow cell, and collection fiber was always very important to the SNR. In addition, the use of RIMF might be good for SNR enhancement [16]. Based on these analyses, the four key parameters were further investigated and found to still have room for improvement.

3.1. LED and its coupling style

Besides spectral parameters (λ_{max} and FWHM), light intensity towards the internal channel of the flow cell is the most important factor in selection of an optimum LED. In terms of power, LEDs is divided into two kinds, i.e., ordinary LEDs and HP LEDs. Ordinary LEDs usually have a rate current of 20 mA and chip size of about 0.3 mm × 0.3 mm. HP LEDs can have a radiant power of 700 mW or above, but their chip size was about 2 mm × 2 mm [9]. If the LED was used in conjunction with a small diameter optical fiber, the coupling efficiency of an HP LED might result in no significant gain over that of an ordinary LED, because it depends on the light intensity per unit area of the chip, rather than the whole radiant luminous flux [17]. Small encapsulation diameter and high light intensity of an LED are beneficial for the increase of light intensity at the detection area. Therefore, the smaller the divergence angle, the higher the light intensity at the detection area, and the higher the fluorescence signal. Small divergence angle also produces less scattering light to the collection fiber, which was brought to low background noise. Two LEDs were then selected, i.e., OSB56L3131A (OptoSupply Corp., Hong Kong, China) and NSPB300B-E (Nichia Corp., Tokyo, Japan) for testing. The detailed parameters of OSB56L3131A were: λ_{max} 470 nm, FWHM 25 nm, power dissipation 20 mA × 3.1 V, 50% power angle 30°, diameter 3 mm, and typical light intensity 8400 mcd, while the detailed parameters of NSPB300B-E were: λ_{max} 470 nm, FWHM 25 nm, power dissipation 20 mA × 3.2 V, 50% power angle 15°, diameter 3 mm, and typical light intensity 6550 mcd. Fig. 2 showed directivities of the two kinds of LEDs. Contrastive experimental results were shown in Fig. 3a and b. The detector SNR produced by OSB56L3131A was a little higher than that by NSPB300B-E. Therefore, the OSB56L3131A was used throughout the following study.

If an LED is coupled to an optical fiber of small diameter, the best coupling is achieved by removing most of the dome of the LED to 0.5 mm or thinner close to the chip, and coupling the fiber directly on the flat surface [17]. The theory was only applicable to

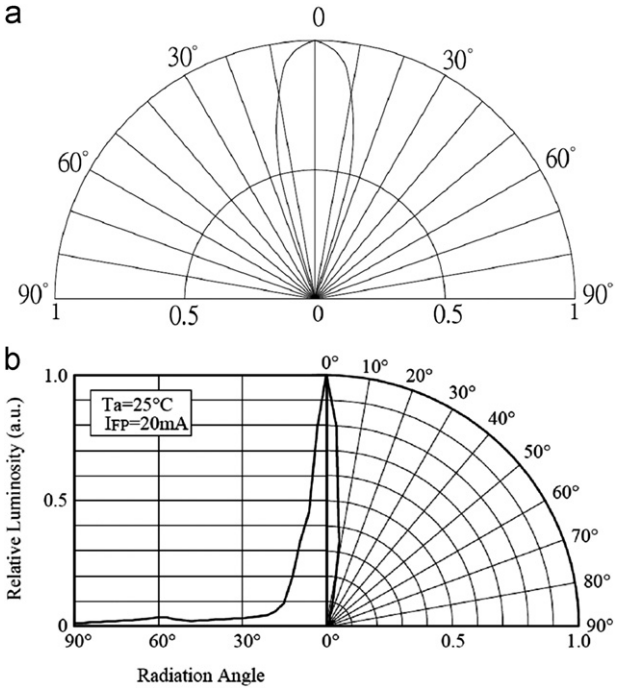

Fig. 2. Directivities of the two kinds of optimum LEDs: (a) OSB56L3131A and (b), NSPB300B-E.

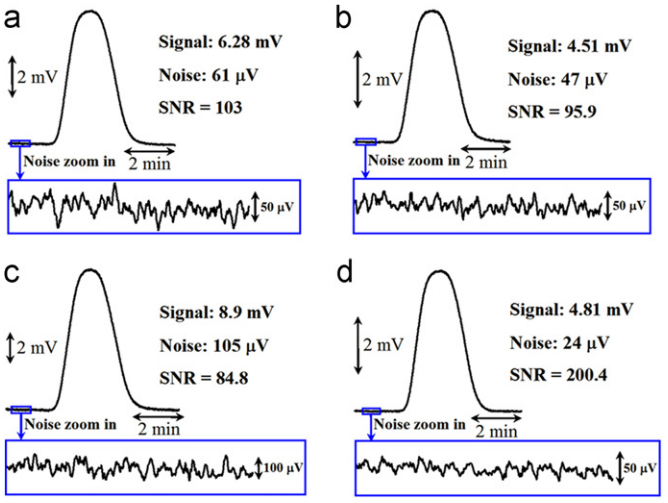

Fig. 3. Experimental results obtained by various schemes. Sample concentration: 10 nM. (a) OSB56L3131A; (b) NSPB300B-E; (c) OSB56L3131A with ball lens and (d) OSB56L3131A with glycerol. Conditions: flow rate 10 μL/min; injection volume 10 μL and PMT voltage 480 V.

the coupling of light power. When moving to LED-FDs in which the SNR should be respected for, the situation was different. The attendance of excitation filter would enhance the SNR to about four times [12,18]. Because the beam divergence angle of the dome-removed LEDs was about 180°, its light beam became highly divergent after passing through the 3 mm thick excitation filter. If an optical fiber or a pinhole of small diameter was coupled, the coupling efficiency of the dome-removed LEDs might be not higher than that of un-removed ones, and so might the fluorescence signal. Moreover, the large divergence angle of the dome-removed LEDs could result in high background noise. Therefore, for LED-FDs, the dome-removal method might reduce the system SNR. In this study, the dome of LED was not removed. Considering the LED had a narrow beam angle of 30°, a ball lens (material K9, refractive index 1.52, diameter 2 mm) coupling was introduced [17]. The whole radiant light power of excitation light passing through the pinhole increased to 2.5 times higher by using the ball lens, but resulted in a slight degradation of the LOD of the detector. The result is shown in Fig. 3c. The reason was as follows. The use of a ball lens increased the divergence angle of the excitation light beam to about 60°, which brought to weaker light intensity towards a unit area away from the pinhole, such as the inside channel of the detection flow cell. Besides, the increased irradiation area on the detection window might result in a higher background noise. The two aspects worked together leading to a slightly higher LOD. In view of these problems, we did not use a ball lens in following experiments. The LED, excitation filter and pinhole were in direct contact with each other, without any other coupling.

3.2. Pinhole diameter

Rectangular and circular shapes of pinhole had been fabricated for investigation. Regardless of the shape of the pinhole, if only the pinhole size was at its optimal, the sensitivity of the detector was similar [9]. A round pinhole was preferred for its easy fabrication. The 3D analysis on SNR had to be considered in radial and axial directions of the flow cell. In the radial direction, there was a plane which was a usual research object. It was vertical to the flow cell and passed through the center of the pinhole. Fig. 4a shows a top view of the optical model of the pinhole, flow cell, and collection fiber; the investigated plane is marked as A–A. Its relevant cutaway view is shown in Fig. 4b. In the plane A–A

(Fig. 4b), it is found that the excitation light effect on the detector SNR depended on its emission position on the pinhole diameter and its divergence angle together. The Fresnel refraction law is

$$\frac{\sin(\theta_1)}{\sin(\theta_2)} = \frac{\eta_2}{\eta_1}, \quad (1)$$

where θ_1 is the incidence angle, θ_2 is the refractive angle, η_1 is the refractive index of incidence media, and η_2 is the refractive index of refractive media. According to the Fresnel refraction law (1), calculated by ray tracing method, when the pinhole diameter is bigger than 240 μm, excitation light passing through that area cannot irradiate the flow cell i.d. area to excite fluorescence signal, as illustrated in Fig. 4b. It travels directly to the collection fiber to increase background noise. The optimal pinhole diameter would be ≤ 240 μm if the radial direction only was considered. However, when the model is upgraded to 3D space where the axial direction is also considered, the situation is changed. In axial direction, the length of detection window is 3 mm instead of 325 μm as in radial direction. As shown in Fig. 4a, part of the excitation light passing through the pinhole area with diameter larger than 240 μm will travel directly to the collection fiber to produce background noise (blue arrow), and part of it can still irradiate the flowcell i.d. area to yield a fluorescence signal (green arrow). But its excitation position is away from plane A–A. If the pinhole diameter is slightly bigger than 240 μm, the increase in background noise is not very significant. Its excitation position is not far away from plane A–A, which is not very difficult for fluorescence signal collection. Thus, the fluorescence signal it produces is higher than the noise, which is good for SNR enhancement. Otherwise, the result will be the contrary. So, there is an optimal pinhole diameter which could compromise the two factors.

In the experiment, the diameter of the pinhole was tested from 200–500 μm, and an optimal value of 350 μm was found, as shown in Fig. 4c. This result validated the theoretical analysis above.

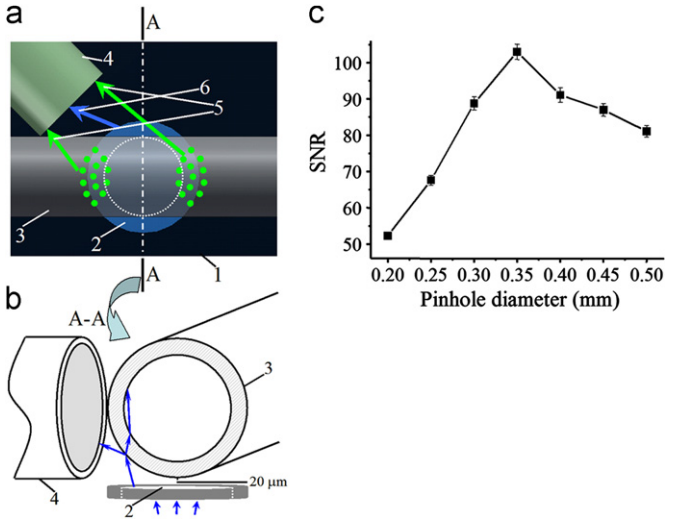

Fig. 4. Theoretical analysis and experimental result of the pinhole diameter effect on system SNR. (a) Top view of the optical model of pinhole, capillary flow cell, and collection fiber; (b) relevant cutaway view of section A–A in (a); and (c) SNR varied with pinhole diameter. Sample concentration: 10 nM. Conditions were the same as in Fig. 3. (1) light tight adhesive tape; (2) pinhole; (3) detection window; (4) collection fiber and (5) fluorescence signal produced by fluorescence molecules excited by excitation light passing through the pinhole area with diameter ≥ 240 μm and (6) background noise produced by excitation light passing through the pinhole area with diameter ≥ 240 μm.

3.3. Calibration

Since the detection area was three-dimensional (3D), a calibration should be considered from the 3D perspective. In our system, the whole excitation module was installed on a 3D displacement adjustable platform. The detection module to fix capillary and collection fiber was fixed on the optical platform by brackets. For calibration of 3D space, two directions were considered, i.e., horizontal and vertical. In the horizontal direction, the flow cell and the collection fiber should be as close as possible but not in physical contact. The projection of the axis of the flow cell on light tight adhesive tape should pass through the center of the pinhole. The extended line of the collection fiber should also pass through the center of the pinhole. In the experiment, these principles were achieved by finely adjusting the 3D displacement platform. A portable 80 × microscope objective was employed for a magnified top view. The actual calibration effect is shown in Fig. 5a. It seemed that a slight movement of the pinhole along the flow cell towards the collection fiber should be favorable for SNR enhancement. We tested the idea and unexpectedly found no improvement on SNR. Equally important, in the vertical direction, the flow cell and the collection fiber should be coplanar, and at the same height from the ground. It was achieved by changing the film thickness. Films of various thicknesses were placed under the flow cell and collection fiber to adjust their heights. An observation channel on the side of the detection module was fabricated for a clear eye view, magnified by the 80 × microscope objective. The relevant actual calibration effect is shown in Fig. 5b.

3.4. RIMF

The addition of RIMF at the detection area could lower both the fluorescence signal and noise level. It had been demonstrated that, for the optical fibers system, the attendance of RIMF could enhance the SNR to about two times [16]. The optical lenses system was unsuitable for the application of RIMF which eliminated the focusing effect of lenses and resulted in a fall of sensitivity. In our pinhole and fiber system, a drop of glycerol was employed to function as the

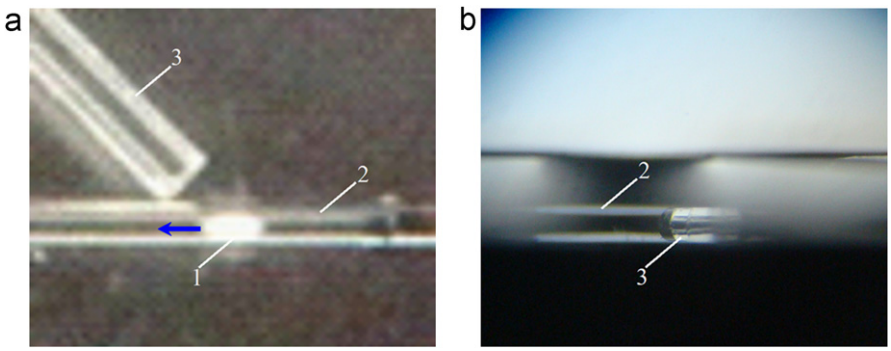

Fig. 5. Figures of actual calibration effects. (a) Horizontal direction and (b) vertical direction. (1) pinhole; (2) detection window and (3) collection fiber.

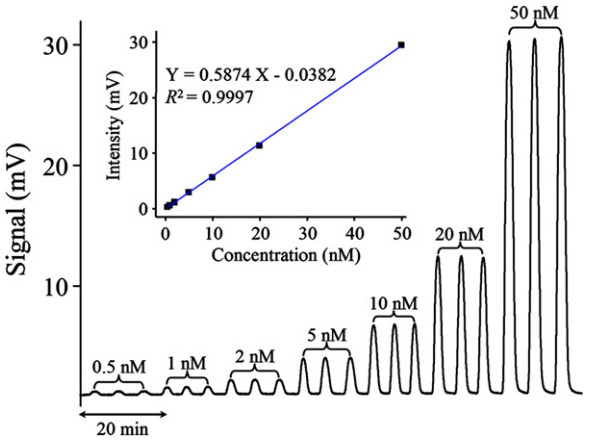

Fig. 6. Linear response of sodium fluorescein (0.5–50 nM) in flow injection mode. Conditions were the same as in Fig. 3.

Table 1
Performance summary of the new detector.

Analyte	LOD (nM)	Linearity range (nM)	Correlation coefficient (R^2)	Peak height R.S.D. (%)	Reproducibility R.S.D. (%)
Sodium fluorescein	0.15	0.5–50	0.9997	2.0	2.2

RIMF. It immersed the detection area adequately. The experiment result is shown in Fig. 3d. From the figure, the use of glycerol brought 1.9 times SNR enhancement.

3.5. System characteristics

The performance of the improved LED-FD was evaluated in terms of the repeatability of peak heights, reproducibility, response linearity, and the limit of detection (LOD) by FIA method. The sample was sodium fluorescein, which is a common fluorescence probe used to evaluate the performance of a fluorescence detector. The error of repeatability was within 2.0% R.S.D. on the peak height in a six-repeated injection of 10 nM solution. The R.S.D. of reproducibility of the reassembling detector was 2.2%. The system exhibited a linear response in the concentration range of 0.5–50 nM, and the correlation coefficient was 0.9997, as shown in Fig. 6. From Fig. 3d, the LOD (SNR=3) of our improved detector was estimated to be 0.15 nM, which was only 1/5 of our latest report [14]. The size of the whole detector was only 9 cm × 9 cm × 4 cm ($W \times L \times H$). Data shown in Table 1 summarizes the performance of the new LED-FD.

For application, the improved LED-FD was combined with an Agilent 1200 Series HPLC system. Fig. 7 shows the chromatogram of four FITC-labeled amino acids detected by the LED-FD. The LOD on the improved LED-FD were 5.0×10^{-10} M, 5.7×10^{-10} M, 6.8×10^{-10} M, and 4.5×10^{-10} M for Arg, Val, Leu and Phe, respectively. These LODs were about five times higher than those on a commercial Agilent G1321A FLD (fluorescence detector) which employs a xenon lamp, pulse modulated technique, lock-in amplifier, low pass filter and reference system.

4. Conclusions

To further enhance the SNR of the compact LED-FD, four key parameters were investigated and optimized, i.e., LED and its coupling style, the pinhole diameter, calibration, and RIMF.

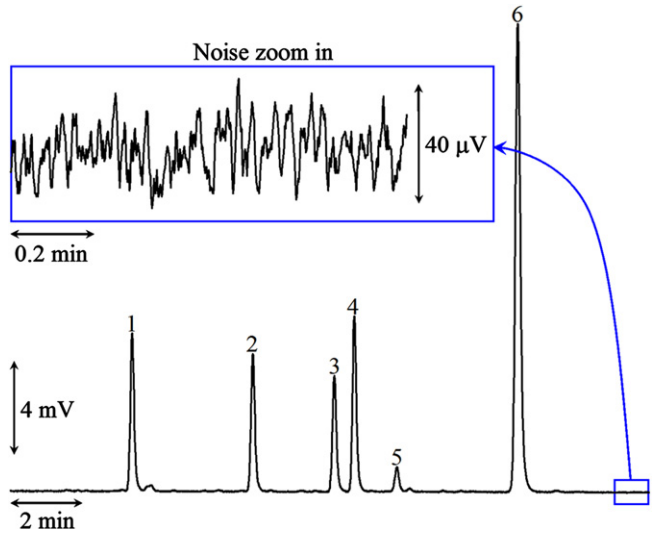

Fig. 7. HPLC chromatogram of FITC-labeled amino acids detected by the improved LED-FD. Sample concentration: 3×10^{-8} M. Peak identification: (1) FITC-labeled arginine; (2) FITC-labeled valine; (3) FITC-labeled leucine; (4) FITC-labeled phenylalanine; (5) impurity and (6) excess FITC.

The LOD of 0.15 nM on the improved LED-FD was obtained without increasing the volume and complexity of the system. Although the improved parameters themselves were not novel, for each parameter a theoretical analysis was given and matched well with the experimental result. The LOD of 0.15 nM was next to the lowest among literatures. The advantages of miniature and integrated LED-FDs are of significance to micromation and integration of LED-FDs which may promote their applications in commercial analytical instruments in the future.

Acknowledgments

This work was supported by the National Natural Science Foundation of China (Grant no. 20635010), Chinese Academy of Sciences, (no. KZCX1-YW-14-3), and the Ministry of Science and Technology of China on High Tech Program (no. 2008AA09Z110).

References

[1] K. Tsunoda, T. Yagasaki, S. Aizawa, H. Akaiwa, K. Satake, Anal. Sci. 13 (1997) 757–764.
[2] S.L. Wang, X.J. Huang, Z.L. Fang, P.K. Dasgupta, Anal. Chem. 73 (2001) 4545–4549.
[3] X.W. Chen, J.H. Wang, Talanta 69 (2006) 681–685.
[4] Roithner Lasertechnik GmbH, Data, Diverse LEDs. Available from: 〈http://www.roithner-laser.com/led_diverse.html#uv〉.
[5] OSRAM Opto Semiconductors GmbH, Data, Product catalog. Available from: 〈http://catalog.osram-os.com/catalogue/catalogue.do?favOid=00000001000222c400e70023&act=showBookmark〉.
[6] A.E. Bruno, F. Maystre, B. Krattiger, P. Nussbaum, E. Gassmann, Trends Anal. Chem. 13 (1994) 190–198.
[7] S. Hillebrand, J.R. Schoffen, M. Mandaji, C. Termignoni, H.P.H. Grieneisen, T.B.L. Kist, Electrophoresis 23 (2002) 2445–2448.
[8] F. Yang, X.C. Li, W. Zhang, J.B. Pan, Z.G. Chen, Talanta 84 (2011) 1099–1106.
[9] E.P. de Jong, C.A. Lucy, Analyst 131 (2006) 664–669.
[10] F. Huo, H.Y. Yuan, X.P. Yang, M.C. Breadmore, D. Xiao, Talanta 83 (2010) 521–526.
[11] F. Huo, H.Y. Yuan, M.C. Breadmore, D. Xiao, Electrophoresis 31 (2010) 2589–2595.
[12] J. Xu, Y. Xiong, S.H. Chen, Y.F. Guan, Talanta 76 (2008) 369–372.
[13] E.P. de Jong, C.A. Lucy, Anal. Chim. Acta 546 (2005) 37–45.
[14] X.H. Geng, D.P. Wu, Y.F. Guan, Talanta 88 (2012) 463–467.
[15] J.L. Fu, Q. Fang, T. Zhang, X.H. Jin, Z.L. Fang, Anal. Chem. 78 (2006) 3827–3834.
[16] J. Xu, S.H. Chen, Y. Xiong, B.C. Yang, Y.F. Guan, Talanta 75 (2008) 885–889.
[17] P.K. Dasgupta, I.Y. Eom, K.J. Morris, J.Z. Li, Anal. Chim. Acta 500 (2003) 337–364.
[18] B.C. Yang, H.Z. Tian, J. Xu, Y.F. Guan, Talanta 69 (2006) 996–1000.